Original Research Article

Multi-component plasma fluid approach to sparking enhanced burns as a complication of diathermy

Marija Radmilovic-Radjenovic*, Branislav Radjenovic

Institute of Physics, University of Belgrade, Pregrevica, Belgrade, Serbia

*Correspondence:
Dr. Marija Radmilovic-Radjenovic,
E-mail: marija@ipb.ac.rs

ABSTRACT

Background: The effects of electric currents flowing through a human body vary from no perceptible to severe tissue injury caused by the electrosurgical spark. Although modern electrodes have been designed to minimize this complication, it was reported that burns have accounted for 70% of the injuries during electro surgery. Some risks of complications depend on a surgeon's knowledge of instruments and safety aspects of technical equipment. The use of alcohol and spirit-based skin preparation solutions brings another risk of burn injuries.

Methods: Apart from the experimental methods, computer modelling is shown to be an effective approach to improve the performance of electrosurgical procedure. The benefits of simulation assisted electro surgery include no ethical approval, low cost, safe and the most important removing conditions that may lead to tissue burns. Here, the onset of sparking between the electrosurgical electrodes has been studied by using the multi-component plasma fluid model.

Results: It was found that the electrode shape significantly affects the sparking formation. The minimum voltage required for sparking has been achieved for cylinder-cylinder configuration, while for other arrangements breakdown voltages are higher. Electrical sparks do not occur equally in both directions between active and passive electrodes due to electrical asymmetries.

Conclusions: This study is dealing with application of multi-component plasma fluid model in simulating sparks produced between electrosurgical electrodes of various shapes, materials and dimensions. Our simulation model offers substantially greater physical fidelity as compared to simulators that use simple geometry. The obtained results are applicable for prevention of potential complications during diathermy procedure.

Keywords: Burns, Diathermy, Multi-component fluid model, Tissue

INTRODUCTION

Diathermy is a therapeutic treatment commonly used in modern day surgery for muscular and joint associated pains.[1,2] The term diathermy means producing heating directly in the tissue of the body stimulating the circulation, accelerating healing, enhancing recovery or relieving the pain.[3] Diathermy plays an integral part in most operations frequently used on a regularly by surgeons of all specialties. Although diathermy procedure is recognized as an invaluable and safe aid in modern surgery, there are reports that burns and electric shocks are worryingly common among patients where diathermy is used to cut tissue and coagulate blood.[4,5] To avoid complications of this kind, computational and simulation methods brought an improvement in studying the design of the electrodes that will cause minimal tissue damage during diathermy. Diathermy uses the heating effect of

passing an electrical current across a resistor which is, in practice, the patient's skin or other tissue being cauterized or cut. Although the incidence of electrosurgical injuries related to diathermy has been reported, it is difficult to comprehend the true impact on the patient body.[6-9] A potential difference produced by the diathermy device generates a current that passes through the patient to complete an electrical circuit unipolar or bipolar. In unipolar diathermy, the cathode represents diathermy tool tip, while the anode is the ground or return plate10. In bipolar diathermy, a very closely spaced cathode and the anode are embedded in a forceps.[10] Thus, a grounding plate is not required with bipolar diathermy and the current pathway is very small. Since resistance and the heating effect are higher where the current passes over a narrow pathway, the current density is very high at the point of the unipolar diathermy pencil tip and relatively low throughout the patient's body and across the large surface area of a correctly placed ground electrode pad. The only significant point of resistance (heat production) should be at the electrode tip.

Depending on the application the electrodes can be in a variety of shapes and sizes. The shape varies from metal plates, rigid metal electrodes, coil or cable electrodes, loop, and ball electrodes to needle electrodes. Regarding electrode size, if the electrodes are too small the diameter of the treated part line of force will be concentrated superficially. When the electrodes are remarkable larger, however, the line of force will be lost in the air. Ideally, the electrodes should be slightly larger than the treated area. To concentrate heat, the electrode should be unequal in size so that a smaller electrode is placed over the area where the concentration of heat is required.

In this paper we are dealing with application of multi-component plasma fluid model to improve fundamental understanding of the sparking enhanced burns during diathermy. The mechanism of the sparking produced between electrodes has been studied by using software package COMSOL multiphysics base on the multi-component plasma fluid model.[11] The focus was put on determination of the breakdown voltage required for the onset of sparking as well as the location where it occurs. Although the shape of the electrodes determines the location where sparking occurs, various angles on the top of the cone electrode do not have a large effect on sparking formation. In addition, the effects of the electrical asymmetries and temperature on the breakdown voltage and the heat transfer have also been estimated.

METHODS

This study contains results obtained by using COMSOL multi physics modeling environment that includes all of the functionality of the DC Discharge and Capacitive Coupled Plasma interfaces. Since the COMSOL simulation package has been described in detail in numerous publications, only the most important facts for this study will be provided here.[12,13] Electron transport is followed by a pair of drift-diffusion equations, one for the electron density and another for the electron energy.[13]

$$\frac{\partial}{\partial t}\left(n_e\right)+\nabla\cdot\left[-n_e\left(\mu_e\bullet\mathbf{E}\right)-\mathbf{D}_e\bullet\nabla n_e\right]=R_e,\,(1)$$

$$\frac{\partial}{\partial t}\left(n_e\right)+\nabla\cdot\left[-n_e\left(\mu_e\bullet\mathbf{E}\right)-\mathbf{D}_e\bullet\nabla n_e\right]+\mathbf{E}\cdot\Gamma_e=R_\varepsilon,\,(2)$$

With the electron diffusivity $\mathbf{De}$, energy mobility μ_ε and energy diffusivity $\mathbf{D}\varepsilon$ are expressed via electron mobility μ_e [13]:

$$\mathbf{D}_e=\mu_eT_e,\;\mu_\varepsilon=\left(5/3\right)\mu_e,\;\text{and }\mathbf{D}_\varepsilon=\mu_\varepsilon T_e.\,(3)$$

The electron source term *'Re'* is expressed as:

$$R_e=\sum_{j=1}^{M}x_jk_jN_nn_e,\,(4)$$

Where 'x_j' represents the mole fraction of the target species for reaction 'j' with the rate coefficient 'k_j', while 'N_n' is the total neutral number density. The rate coefficients can be calculated from cross section data 'σ_k':

$$k_k=\gamma\int_0^\infty\varepsilon\sigma_k\left(\varepsilon\right)f\left(\varepsilon\right)d\varepsilon,\,(5)$$

Where '$\gamma=(2q/me)^{1/2}$', 'm_e' is the electron mass, while 'ε' and 'f' are the electron energy and the electron energy distribution function, respectively. The electron energy loss can be expressed as a sum of the collisional energy loss over all reactions:

$$R_\varepsilon=\sum_{j=1}^{P}x_jk_jN_nn_e\Delta\varepsilon_j,\,(6)$$

Where '$\Delta\varepsilon_j$' represents the energy loss from reaction 'j'.

One of the most complicated steps in the finite element calculations is the meshing. Meshing involves volume separation into many smaller elements affecting the computational time and accuracy of the obtained results.[12] generating a structured mesh in default mesher is not an easy task. COMSOL multi physics allows a wide selection of tools to control and generate mesh: mapped, unstructured quad, triangular, tetrahedral, swept, and boundary layer. To achieve high-quality calculations, we have applied triangular mesh and 4-layers of quadrilateral elements to cover the whole geometry and boundaries, respectively. The division of the domains can be considered to be quite uniform, with a small change of the distribution of the elements in the vicinity of the electrode curve. This study contains results of simulations performed from February 2020 to July 2020.

RESULTS

At the beginning, we performed test calculations with the available experimental data. Breakdown voltage curves for various: a) electrode arrangements and b) dimensions of the cylindrical electrode are shown. As can be seen from (Figure 1a), the best agreement between calculated and measured data (red squares) has been achieved for the cylinder-cylinder electrodes (blue circles). For configurations with one (green diamonds) or two spherical electrodes (brown down triangles), breakdown voltages are higher than those calculated for the cylinder-cylinder electrodes (red circles). It is easier to produce

conditions for sparking with decreasing of the diameter of the cylindrical electrode as demonstrated in (Figure 1b).

Figure 2 exhibits: a) initial electric potential (without plasma) and b) electron density distributions when sparking starts for cylinder-cylinder, sphere-sphere and cone-cone electrode arrangements. It is clear from Figure 2b the geometry of the electrodes strongly affects the location where sparks getting started. In Figure 3 Similarities a) electric potentials and b) the onsets of sparking for configuration composed of two equal cone electrodes are shown. As can be observed, various angle on the top of the tip does not have a large effect on sparking formation.
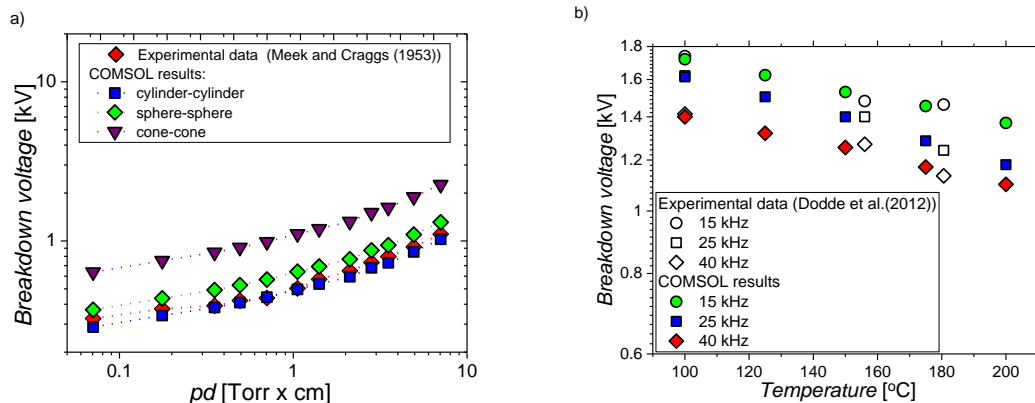

Figure 1: The breakdown voltage curves for various: a) electrode configurations (cylinder-cylinder, sphere-sphere, and cone-cone) and b) temperature for various frequencies.
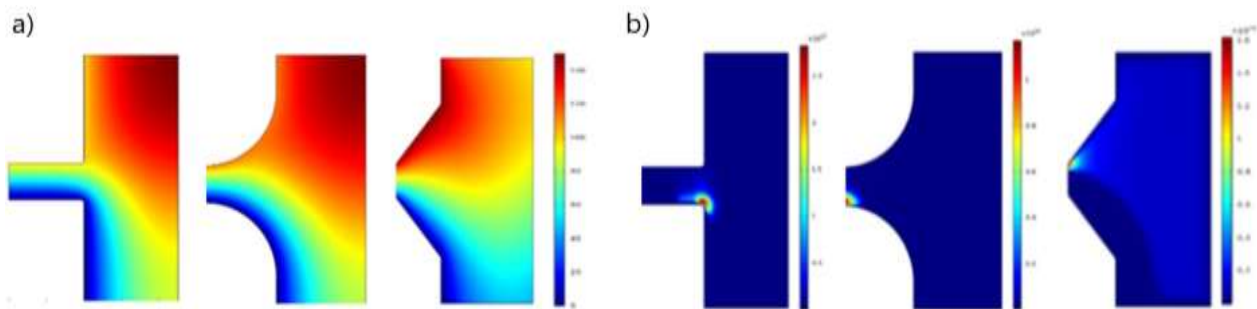

Figure 2: (a) Electrical potential at t=0 and (b) electron density illustrating the onset of sparking for cylinder-cylinder, sphere- sphere and cone-cone configurations.
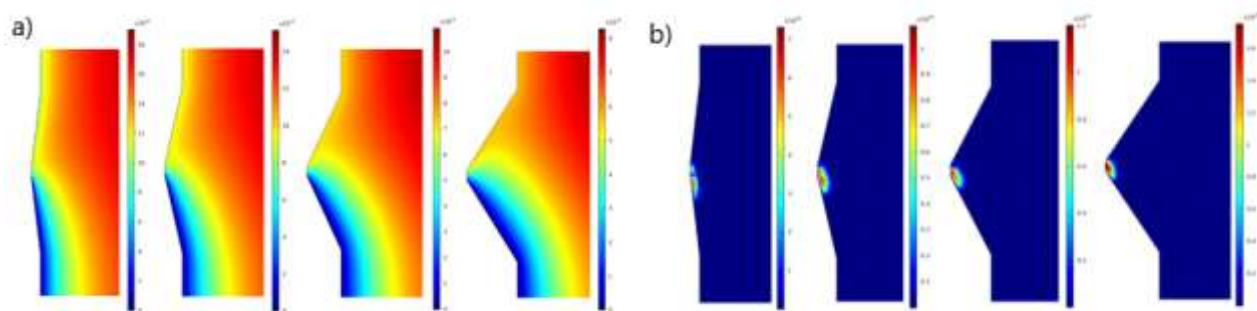
Figure 3: (a) Electrical potential at t=0 and (b) electron density demonstrating locations where sparking begins for cone-cone electrodes with various angle on the top of the tip.
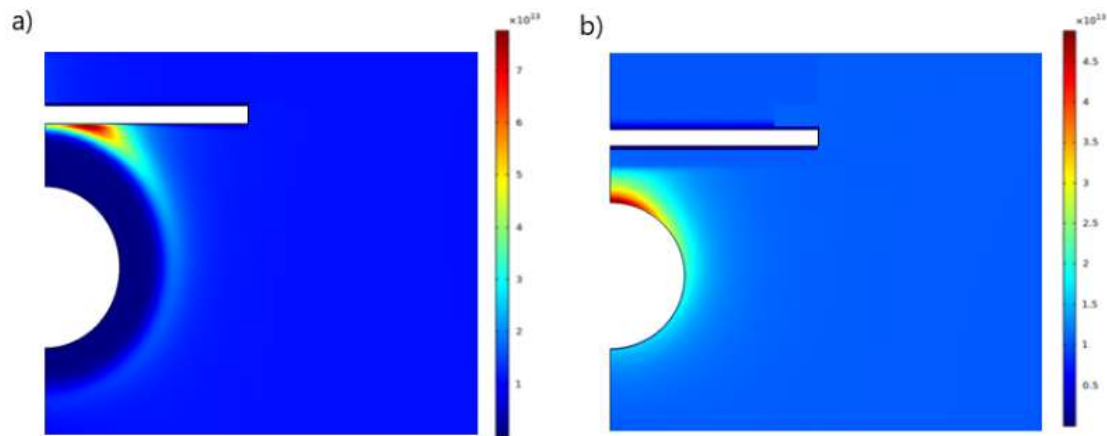
Figure 4: Sparking occurring between spherical metallic electrode and the metal plate which is: a) positive and b) negative.
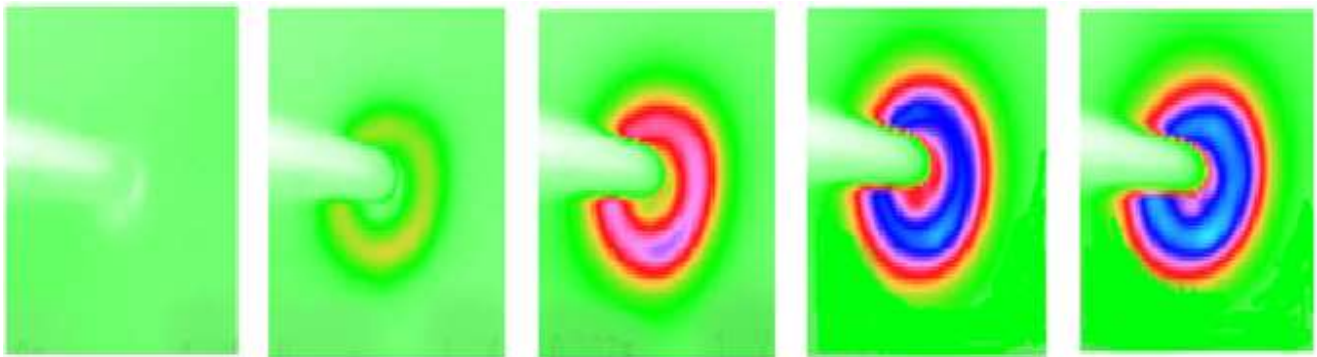
Figure 5 Simulation results illustrating thermal characterization of tissues.

Locations where sparking takes place in the case of the positive and negative cycles are illustrated in (Figure 4). In both cases, the electric field is neither uniform nor symmetrical and not affected by the presence of an organic tissue.

An accurate understanding of heat transfer and temperature mono polar electrode, the finite element method is applied in order to solve forward transient heat transfer problem. Simulation results on Figure 5 show that the temperature increase leads to the heat increase, indicating that vaporization plays an important role in energy dissipation through latent heat loss. Effect on the tissue during diathermy allow us to predict areas of tissue damage. For that purpose, the knowledge of the tissue thermal properties including specific heat and thermal conductivity is needed. Based on the measured data regarding the tissue surface temperature for mono polar electrode, the finite element method is applied to solve forward transient heat transfer problem. Simulation results on (Figure 5) show that the temperature increase leads to the heat increase, indicating that vaporization plays an important role in energy dissipation through latent heat loss.

DISCUSSION

This paper contains results of simulation studies of the onset of sparking which leads to the delivery of energy to the tissue and causing burns. For that purpose, calculations were carried out for various electrode arrangements representing surgical electrodes using COMSOL Multi physics based on the multi-component plasma fluid model. Sparking is analyzed through breakdown voltage characteristics including electric potential and electron density distribution.[14-18] The influence of the electrode configuration and the temperature on the breakdown voltage has been considered. The breakdown voltage curves for all configurations follow standard scaling law. Results obtained for cylinder-cylinder configuration shows the best agreement with the experimental data. Although have the same tendencies, the breakdown voltages for sphere-sphere and cone-cone electrodes are significantly higher implying that sparking conditions are easily to achieve for cylinder-cylinder configuration. The breakdown voltage decreases with increasing the temperature. Furthermore, sparking does not occur equally in both directions between active and passive electrodes introducing electrical asymmetries a

consequence of the non-symmetry of the electric field generated between them.

The basic mechanism of tissue ablation and dissection in electro surgery involves Joule heating of the conductive tissue by an electric current which leads to vaporization and ionization of the water content in the tissue adjacent to the electrode, and ultimately to vapor expansion and tissue fragmentation.[19,20] Tissue heated below the vaporization threshold remains in place but can undergo thermal denaturation, with its extent determined by the temperature levels and duration of the hyperthermia. The depth of heat penetration into tissue is determined by the distribution of electric field (source of heating) and by thermal diffusion. Thus, to confine the collateral damage zone in tissue, both of these factors should be minimized. Presented simulation results could be useful not only for understanding the sparking mechanism but also for preventing burns due to complications of diathermy procedures.

CONCLUSION

This contains results of the simulation studies of the sparking between electrosurgical electrodes that enhances skin burns during diathermy. Calculations were performed by using the COMSOL software package that applied a multi-component fluid model. For test calculations, simulation conditions were generally based on the experimental conditions. The overall divergence between simulation and experimental results is less than 7% confirming that the COMSOL Multi physics can be successfully applied in studying sparking as the origin of skin burns. However, some initial conditions may bring problems. For example, if the initial electron density is too low then the plasma may not be able to sustain. If the initial electron density is too high then convergence problems may occur during initial time steps.

The minimum voltage required for sparking is obtained for the arrangements composed of two cylindrical electrodes. For a configuration with two spherical or conical electrodes, breakdown voltages are higher. On the other hand, it seems that sparking occurs at a similar location regardless of the angle on the top of the tip. It is also evident that the electrical sparks do not occur equally in both directions between the active electrode and the passive metal plate due to electrical asymmetries. Although asymmetry in the breakdown voltages does not occur between electrodes of the same materials and shape, replacing one of the electrodes by a larger sphere or a metal plate gradually increases the asymmetry. Since asymmetry is the cause of undesirable direct current burns fundamental knowledge of the sparking phenomena is crucial for ensuring patient safety. In addition, it was shown that the temperature increase leads to the heat increase, indicating that vaporization plays an important role in the energy dissipation through latent heat loss. Presented simulation results could be useful not only for understanding the sparking mechanism but also for

preventing burns due to complications of diathermy procedures.

REFERENCES

1. Boyd DE, Palmer JHM. Surgical diathermy. Anaesthesia & Intensive Care Medicine. 2013;14(10):P431-3.
2. MacG Palmer JH. Surgical diathermy and electrical hazards: causes and prevention. Anaesthesia & Intensive Care Medicine. 2016;17(10):P480-85.
3. Fu T, Lineaweaver WC, Zhang F, Zhang J. Role of shortwave and microwave diathermy in peripheral neuropathy. J Int Med Resea. 2019;47(8):3569-79.
4. Vedovato JW, Polvora VP, Leonardi DF. Burns as a Complication of the Use of Diathermy. J Bur Care Rehabilit. 2004;25(1):120-3.
5. Dewey WS, Cunningham KB, Shingleton SK, Pruskowski KA, Welsh AM, Rizzo JA. T2 Safety of Early Post-operative Range of Motion in Burn Patients with Newly Placed Hand Autografts. J Bur Care Rese. 2020;41(4):809-13.
6. McQuail PM, McCartney BS, Baker JF, Kenny P. Diathermy awareness among surgeons-An analysis in Ireland. Annals Med Surg. 2016;12(12):54-9.
7. Gibs P. Diathermy burns in the mouth. Two case reports. Austr Dent J. 1985;30(4):296-7.
8. Aigner N, Fialka C, Fritz A, Wruhs O, Zöch G. Complications in the use of diathermy. Burns 1997;23(3):256-64.
9. Demircin S, Aslan F, Karagoz YM, Atilgan M. Medicolegal aspects of surgical diathermy burns: a case report and review of the literature. Rom J Leg Med. 2013;21(3):173-6.
10. Tammam AE, Ahmed HH, Abdella AH, Taha SAM. Comparative Study between Monopolar Electrodes and Bipolar Electrodes in Hysteroscopic Surgery. J Clin Diagn Res. 2015;9(11):QC11.
11. COMSOL Multiphysics. Stockholm, Sweden; 2008. Available at: www.comsol.com. Accessed on 5 May 2020.
12. Radmilović-Radjenović M, Radjenović D, Radjenović B. Simulation studies of the electrode configuration effect on the breakdown phenomenon. Int J Advan Resea. Comp Sci Electro Engine. 2019;8(12):68-71.
13. Elshafieya O, Haroon M, Lotfi MA, Moghavvemi M. The Development of Spinal Surgery Training Model. AIP Confer Proceed. 2019;2102:130009.

14. Meek JM, Craggs JD. Electrical breakdown of gases. Oxford, UK: Oxfo Pre;1953.
15. Dias E, Schneider B, Ribeiro E. On the origin of skin burns and neuromuscular electrical stimulation as a consequence of electrosurgical procedures. Resea Biomed Enginee. 2019;35(2):111-22.
16. Dodde RE, Gee JS, Geiger JD, Shih AJ. Monopolar Electrosurgical Thermal Management for Minimizing Tissue Damage. IEEE Transac Biomed Enginee. 2012;59(1):167-73.
17. Lu Z, Arikatla VS, Han Z, Allen BF, De S. A Physics-based Algorithm for Real-time Simulation of Electrosurgery Procedures in Minimally Invasive Surgery. Int J Med Robot Comp Assis Surg. 2014;10:495-504.
18. Radmilović-Radjenović M, Radjenović B. Studies of the origin of skin burns during electrocautery based on multi-component plasma fluid model. J Surg Surgic Rese. 2020;6(1):27-9.
19. Brown DB. Concepts, considerations, and concerns on the cutting edge of radiofrequency ablation. J. Vasc. Interventional Radiol. 2005;16:597-613.
20. Massarweh NN, Cosgriff N, Slakey DP. Electro surgery: History, principles, and current and future uses. J Amer Colle Surge. 2006;202:520-30.